Article

pubs.acs.org/Biomac

Role of Polymeric Endosomolytic Agents in Gene Transfection: A Comparative Study of Poly(L-lysine) Grafted with Monomeric L-Histidine Analogue and Poly(L-histidine)

Hee Sook Hwang,[†,‡] Jun Hu,[†,‡] Kun Na,[§] and You Han Bae*[,‡,∥]

[‡]Department of Pharmaceutics and Pharmaceutical Chemistry, The University of Utah, Skaggs Research Building, Rm 2760, 30S, 2000E, Salt Lake City, Utah 84112, United States

[§]Department of Biotechnology, The Catholic University of Korea, 43 Jibong-ro, Wonmi-gu, Bucheon-si, Gyeonggi-do 420-743, Korea

[∥]Utah-Inha Drug Delivery Systems (DDS) and Advanced Therapeutics Research Center, 7-50 Songdo-dong, Yeonsu-gu, Incheon, 406-840, Korea

Supporting Information

ABSTRACT: Endosomal entrapment is one of the main barriers that must be overcome for efficient gene expression along with cell internalization, DNA release, and nuclear import. Introducing pH-sensitive ionizable groups into the polycationic polymers to increase gene transfer efficiency has proven to be a useful method; however, a comparative study of introducing equal numbers of ionizable groups in both polymer and monomer forms, has not been reported. In this study, we prepared two types of histidine-grafted poly(L-lysine) (PLL), a stacking form of poly(L-histidine) (PLL-*g*-PHis) and a mono- L-histidine (PLL-*g*-mHis) with the same number of imidazole groups. These two types of histidine-grafted PLL, PLL-*g*-PHis and PLL-*g*-mHis, showed profound differences in hemolytic activity, cellular uptake, internalization, and transfection efficiency. Cy3-labeled PLL-*g*-PHis showed strong fluorescence in the nucleus after internalization, and high hemolytic activity upon pH changes was also observed from PLL-*g*-PHis. The arrangement of imidazole groups from PHis also provided higher gene expression than mHis due to its ability to escape the endosome. mHis or PHis grafting reduced the cytotoxicity of PLL and changed the rate of cellular uptake by changing the quantity of free ε-amines available for gene condensation. The subcellular localization of PLL-*g*-PHis/pDNA measured by YOYO1-pDNA intensity was highest inside the nucleus, while the lysotracker, which stains the acidic compartments was lowest among these polymers. Thus, the polymeric histidine arrangement demonstrate the ability to escape the endosome and trigger rapid release of polyplexes into the cytosol, resulting in a greater amount of pDNA available for translocation to the nucleus and enhanced gene expression.

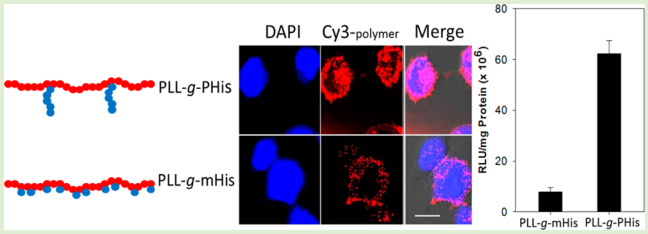

INTRODUCTION

Most polymeric gene carriers gain access to target cells via endocytic pathways and must escape from the endosomes before they merge with the lysosomes, rich in digestive enzymes that degrade the therapeutic genes.[1,2] Polymers synthesized with pH-sensitive groups serve as proton sponges and provide endosomolytic ability that helps escape from the endosome and significantly enhances the potential of gene delivery.[3,4] The "proton sponge effect" underlies a common strategy for endosomal escape in which the high buffering capacity of the gene carrier agents, i.e., proton absorption by carrier protonation, induces an influx of counterions and water into the endosomes.[5−7] The resulting osmotic pressure build-up subsequently leads to rupture of the endosomal membrane and releases the entrapped components into the cytosol.[8,9] However, the proton sponge effect is still under debate, and contradictory reports insist this hypothesis is not the dominant mechanism of endosomal escape.[10−12] Benjaminsen et al. has argued that polymer concentration inside the endosomes is not sufficient to generate the necessary osmotic gradient to facilitate polyplex escape from the endosomes.[13] Many other papers do not rule out the proton sponge effect, but have proposed a charge density of polymer that affects the interaction with the endosomes and may destabilize the endosomal membrane inducing membrane disruption, thinning, and erosion to facilitate the polyplexes escaping from the endosomes.[11,14]

Histidine (His) analogues having imidazole group grafted to various polymers including PLL[15] and gluconic acid[16] have become popular materials to deliver pDNA. A study conducted by Singh et al. showed that conjugating histidine, which has a pK_a near endosomal pH, provided effective buffering for strong endosomolytic activity in the endosomal compartments,[17] increased endosomal escape,[18,19] and enhanced the transfection efficiency and gene expression.[20,21] The protonation state of the

Received: June 9, 2014
Revised: July 31, 2014
Published: August 21, 2014

imidazole group is determined by a lone electron pair of the unprotonated nitrogen atom in the imidazole ring of the His analogues, which has a pK_a around 7.[22] Poly(L-histidine) (PHis), known as an effective pH-buffering and endosomal pH targeting agent,[23,24] has been developed and applied for more than a decade as a component of pH-sensitive polymeric carriers. When introduced into the early endosomes, the micelles containing PHis blocks demonstrate strong endosomolytic activity and the ability to produce therapeutic cytosolic drug concentrations in a relatively short time period.[22,25,26] These properties have led us to hypothesize that nanocarriers containing PHis blocks result in enhanced gene delivery by inducing endosomal swelling via the proton sponge effect and simultaneously interacting with and disrupting the lipid bilayer membrane of the endosome and facilitating release of the cargo.[25,27,28]

Poly(L-lysine) (PLL) was the first polycationic nonviral vector used for gene delivery[8] numerous variations have been explored for the purpose due to its biodegradability into benign products.[29] However, the high positive charge density of PLL still causes cytotoxicity and prevents the release of plasmid DNA (pDNA) from PLL polyplexes. PLL also lacks endosomolytic activity due to the absence of secondary and tertiary amines which results inasmuch as a 10-fold low transfection efficiency in vitro,[30,31] than a standard branched poly(ethylenimine) (bPEI 25 K) in polymeric gene transfection.[32]

We constructed two histidylated PLLs in this study: PLL modified with monomeric histidine analogue (mHis) (PLL-*g*-mHis) and PLL grafted with short PHis blocks (PLL-*g*-PHis) with an equivalent number of imidazole groups in the two architectures. Shown through this work, we conduct a comparative study of two architectures for gene delivery regarding relative endosomolytic activity and transfection efficiency. We propose that polymers with high positive charge density are capable of binding to the negatively charged endosomal membrane. As the membrane swells due to the increased osmotic pressure, local stress at the point where the polymer is bound can cause the membrane to be disrupted and release the gene cargo into the cytosol.

MATERIALS AND METHODS

Materials. Dimethyl sulfoxide (DMSO), *N*,*N*-dimethylformamide (DMF), 4-(2-hydroxy-ethyl)-1-piperazine (HEPES), 3-(4, 5-dimethylthiazol-2-yl)-2,5-diphenyltetrazolium bromide (MTT), D-glucose, sodium bicarbonate, recombinant human insulin, ethidium bromide (EtBr), heparin sodium salt (139 USP units/mg), paraformaldehyde (PFA), Hoechst 33342, RPMI 1640 medium, Dulbecco's phosphate buffered saline (DPBS), Dulbecco's modified Eagle's medium (DMEM), Poly(L-lysine) hydrogen bromide (PLL·HBr), Cy3-NHs, and FITC were purchased from Sigma-Aldrich (St. Louis, MO). LysoTracker-Red dye and YOYO-1 were purchased from Invitrogen (Carslbard, CA). A firefly luciferase (gWiz-Luc or pLuc) pDNA was bought from Aldevron (Fargo, ND). Rabbit whole blood cells were purchased from Hemostat (Hemostat Laboratories, CA) and dialysis membranes were obtained from Spectrum Laboratories, Inc. (Rancho Dominguez, CA). Boc-His (DNP, dinitrophenyl)−OH·isopropanol (>99%) was purchased from Bachem (U.S.A.).

Synthesis of Boc-Poly(N^{im}-DNP-histidine), Poly(L-lysine)-*graft*-poly(L-histidine) (PLL-*g*-PHis), and PLL-*graft*-monomeric L-Histidine (PLL-*g*-mHis). *Boc-Poly(N^{im}-DNP-histidine).* Before the conjugation with polymers and poly(L-histidine), DNP protected poly(L-histidine) was first prepared according to our previous report.[26] Briefly, the PHis block was prepared by a ring-opening polymerization method using amine-containing small molecules, N-Boc-1,4 butanediamine, as an initiator, and the number-average molecular weight (MW) of PHis was determined to be 3.7 kDa by its ^{1}H NMR spectrum.

Poly(L-lysine)-graft-poly(L-histidine) (PLL-g-PHis). Poly(L-lysine) (100 mg), succinic anhydride (4.1 mg) and DMAP (10 mg) were first dissolved in 10 mL of anhydrous DMSO. After 2 days stirring at 40 °C, the modified poly(L-lysine) was added with NHS (9.4 mg) and DCC (17 mg). After 1 day stirring, Boc-Poly(N^{im}-DNP-histidine) was added into the DMSO solution under nitrogen airflow. Then 2-mercaptoethanol (3 mL) was added after 2 days dropwise into the mixture for overnight stirring. The product was precipitated in ether/ethanol (50:50%, V/V) and purified by dialyzing against DMSO for 2 days and DI water for 2 days with a dialysis membrane of MWCO 3500 g/mol. The final yellow product was obtained after lyophilization, and the yield of the product was 65%.

Poly(L-lysine)-graft-mono-L-histidine (PLL-g-mHis). The synthesis of PLL-*g*-mHis is started with 0.5 g poly(L-lysine) and 0.212 g L-histidine. These materials were dissolved in 30 mL of DI water, and after adjusting the pH to 5.0, 0.262 g EDC·HCl was added to the solution. After stirring the mixture overnight, the solution was dialyzed against deionized water for 2 days with at least four changes using dialysis membrane (MWCO 6000−8000 g/mol). The final product was collected after lyophilization, and the yield of the product was 89%.

Characterization of Polymers. ^{1}H NMR spectra were recorded on a Varian Unity 400 at 9 T with NaLoRAc Z-spec broadband probe for the modified polymers in D_2O/DCl mixed solvent with 10 v% DCl and chemical shifts were given in parts per million from tetramethylsilane.[15] The average number of imidazole molecules bound per polylysine was calculated according to $x = 6 \times h_{8.7}/h_{lys} \times 100\%$, where x was the percentage of imidazole repeat to lysine repeat, $h_{8.7}$ was the value of the integration of the signal at 8.7 ppm corresponding to the proton of histidine, h_{lys} was in the range 1.3−1.9 ppm corresponding to the six methylene protons of lysine residues.

Gel permeation chromatography (GPC) measurement of the PHis was performed on an Agilent 1100 Series high performance liquid chromatography (HPLC) system equipped with a TSKgel G3000HHR GPC column equilibrated at 30 °C and a refractive index detector. DMF with 10 mM LiBr solution was used as the eluent at a flow rate of 1 mL/min for PHis before deprotection.[26]

The buffering capacity of polymers was measured via acid−base titration.[33] Polymers were dispersed in 150 mM NaCl, and pH of solutions was adjusted to 10 using 1 N NaOH. Then the solutions (1 mg/mL, total volume 2 mL) were titrated with 0.1 N HCl to monitor the pH changes of the polymer solution. The proton buffering capacity of polymers was compared at a pH of 7.4 to 5.1 and calculated using the equation below, where ΔV_{HCl} is the volume of HCl that used to titrate the pH, C_{HCl} is the concentration of HCl, which was 0.1 N, and m is the mass of the polymer, which was 2 mg.

$$\text{buffering capacity} = \frac{\Delta V_{HCl} \times C_{HCl}}{m}$$

The membrane-disruptive activity of the difference between PLL-*g*-PHis and PLL-*g*-mHis was measured using a red blood cell (RBC) hemolysis assay.[34] RBCs were harvested by centrifuging whole blood to remove serum and resuspended in 100 mM dibasic sodium phosphate at pH 7.4 and 5.5 at 5×10^8 cells/mL. A total of 200 μL of RBC suspension and 800 μL of buffer solution of polymers were mixed at final concentration of polymers 50 μg/mL and incubated at 37 °C for 1.5 h. Buffer only and deionized water were used as negative and positive control separately. After centrifuge, lysis was determined by measuring the absorbance of the supernatant at 541 nm. The percent hemolysis was calculated by the following formula:

$$\text{hemolysis}(\%) = \frac{\text{Abs}_{\text{sample}} - \text{Abs}_{\text{blank}}}{\text{Abs}_{\text{positive control}}} \times 100$$

Physicochemical Characterization of Polyplexes. A solution of cationic polymers and solution of pDNA (20 μL per 1 μg of pDNA) in HEPES buffer (20 mM, pH 7.4) were prepared separately and mixed to form polyplexes. After 30 min incubation at RT, the prepared

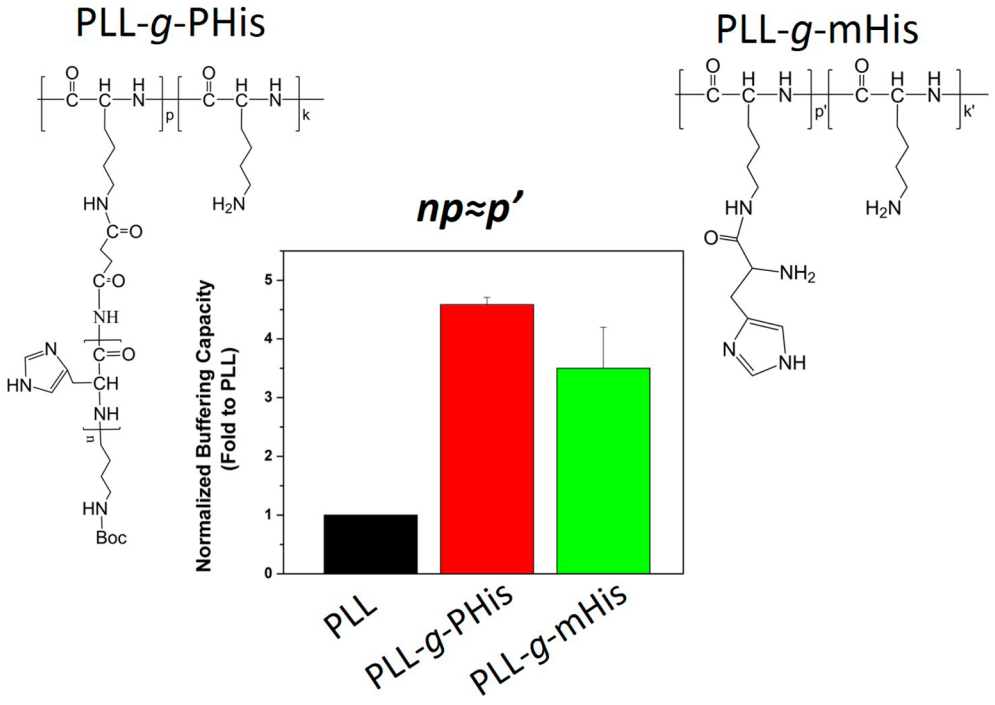

Figure 1. Poly(L-lysine)-*g*-poly(L-histidine) (PLL-*g*-PHis) and poly(L-lysine)-*g*-mono-L-histidine (PLL-*g*-mHis) chemical structures and comparison of buffering capacity.

polyplexes were used for further experiments. Polyplexes were expressed based on the *N*/*P* ratio; the mole ratio of the amines (*N*) of polycation per phosphate group (*P*) of pDNA.

Condensation of DNA (0.5 μg of pDNA) with polymers was monitored using a gel electrophoresis assay. Polyplexes with several complexation ratios were loaded into a 0.8% agarose gel containing ethidium bromide (EtBr), and a constant voltage (95 V) was applied to the polyplex-loaded gel in 0.5xTBE buffer for 40 min. Shielded or exposed pDNA from the polyplexes was detected using a UV illuminator. Polyplexes at *N*/*P* ratio 5 were then prepared in 20 mM HEPES buffer at pH 7.4 and 5.5 followed by incubation in solutions of various heparin (used as the competing polyanion) concentrations at 37 °C for 30 min to monitor the pH-dependent pDNA release. The release of pDNA was analyzed in 0.8% agarose gel containing EtBr (95 V, 40 min). In addition, decomplexation of pDNA from polyplexes was monitored by a YOYO 1-intercalated pDNA containing heparin. Relative fluorescent units (RFUs) of polyplexes was measured using a plate reader at 495 (excitation) and 515 nm (emission). Free YOYO 1-intercalated pDNA and the buffer solution were set as 100 and 0%, respectively, and pDNA release was calculated by the following equation:[30]

$$\text{pDNA release}(\%) = \frac{\text{RFU}_{\text{polyplex}} - \text{RFU}_{\text{buffer}}}{\text{RFU}_{\text{pDNA}} - \text{RFU}_{\text{buffer}}} \times 100(\%)$$

The particle sizes and zeta potential of polyplexes were monitored using a Zetasizer Nano ZS (Malvern Instrument, U.K.) at a wavelength of 677 nm and a constant angle of 90° at RT (25 °C). Polyplexes were diluted in HEPES buffer (20 mM, pH 7.4) with the concentration of pDNA set to 2.5 μg/mL.

Cells and Cell Culture. Hela cells (human cervical carcinoma cell line) were cultured in DMEM supplemented with 10% FBS and D-glucose (4.5 g/L). MCF7 cells (human breast adenocarcinoma cell line) were cultured in RPMI supplemented with 10% FBS, D-glucose (2 g/L), and insulin (4 mg/L). Both cells were grown and maintained under humidified air containing 5% CO_2 at 37 °C.

Biological Characterization of Polymer and Polyplexes. To visualize the localization of Cy3-labeled polymers under a confocal microscope, 1 mL × 2.4 mg/mL DPBS solution of PLL-*g*-PHis, PLL-*g*-mHis, or PLL was mixed with 40 μL × 1 mg/mL DMSO solution of Cy3-NHS separately, after stirring overnight, the mixtures were dialyzed against DPBS for 1 day with two changes using dialysis membrane (MWCO 3500 g/mol). The final concentration of polymers in DPBS almost kept constant at 2.4 mg/mL. For fluorescence labeling with FITC and Cy3 together, 2 mL × 1 mg/mL DPBS solution of PLL-*g*-PHis, PLL-*g*-mHis or PLL was mixed with 40 μL × 1 mg/mL DMSO solution of Cy3-NHS and 60 μL × 1 mg/mL ethanol solution of FITC at the same time, after stirring overnight, the mixtures were dialyzed against DPBS for 1 day with two changes using dialysis membrane (MWCO 3500 g/mol). The final concentration of polymers in DPBS almost kept the same as 1 mg/mL.

The intracellular pH environments of polymers were monitored using fluorescence method, as reported by articles.[35,36] For the construction of pH calibration curve, Hela cells were seeded in six-well plates at a density of 2 × 10^5 cells/well and cultured for 24 h before treatment. After treated with FITC + Cy3-labeled PLL-*g*-PHis and PLL-*g*-mHis 4 h, the cells were suspended in one of four pH clamping buffers (130 mM KCl, 1 mM $MgCl_2$, 15 mM HEPES, and 15 mM MES) with pH adjusted to 5, 5.5, 6, and 7.4. The cells containing fluorescent polymers were monitored using flow cytometry. The correlation between pH and average Cy3/FITC ratios of pH clamp cells was calibrated. Based on the pH calibration curve, the intracellular pH of polymers at different time were calculated.

To determine the polymer cytotoxicity in vitro, a MTT-based cell viability test was performed in 96-well plates as previously reported.[33] Hela and MCF7 cells were seeded at a density of 2 × 10^3 and 5 × 10^3 cells per well and the cells were cultured for 24h in serum containing culture medium (100 μL of medium per well). Different concentration ranges (0−100 μg/mL) of polymers were exposed to the cells for 24 h, then the cells in the culture medium of 0.1 mL were treated with MTT solution (5 mg/mL, 10 μL) to measure cell survival. After 4 h incubation, the culture medium was aspirated and 100 μL of DMSO was added to dissolve the formazan crystals. The absorbance of the solution was monitored at 570 nm using a microplate reader.

YOYO1-labeled pDNA was used to monitor cellular uptake of polyplexes. Cells were treated with 1 μg pDNA (1 mg/mL) per well, and 4 h post-transfection, the cells were washed with DPBS, detached, and fixed using PFA 4% solution. Analysis was performed using a flow cytometry (FACScan Analyzer, Becton−Dickinson; Franklin Lakes, NJ) equipped with a primary argon laser (488 nm) and a fluorescence

dx.doi.org/10.1021/bm500843r | *Biomacromolecules* 2014, 15, 3577−3586

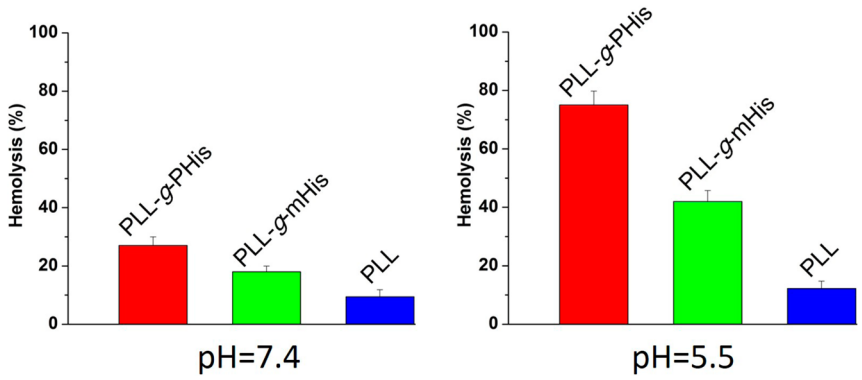

Figure 2. pH dependence of hemolytic activity of PLL-*g*-PHis and PLL-*g*-mHis in pH 7.4 and pH 5.5. Data shown are the mean ± std error; $n = 3$.

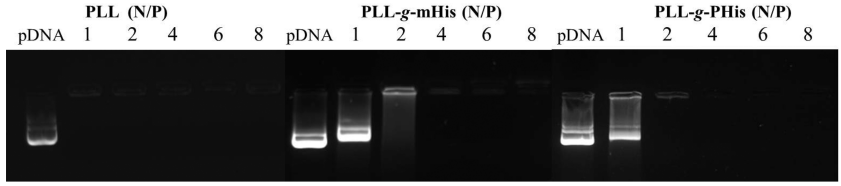

Figure 3. Gene condensation ability of polymers with pDNA in 0.8% agarose gel at 80 V for 90 min.

detector (530 ± 15 nm) for YOYO-1 detection. The uptake of the polyplexes was analyzed through 10000 gated events per sample.

In vitro transfection studies were performed in MCF7 and Hela cells, and both cells were seeded in 6-well plates at a density of 5×10^5 and 1×10^5 cells/well, respectively. After 24 h, the culture medium was replaced with serum-free transfection medium 1 h before the addition of polyplexes. Then the polyplexes (1 μg of pDNA per 20 μL) are transfected in cells and incubated for 4 h, and serum-containing culture medium was added in cells and incubated for additional 44 h. When the transfection experiments were completed, the cells were rinsed with DPBS for twice and then lysed in a reporter lysis buffer. The relative luminescence unit (RLU) was evaluated by luciferase assay kit (Promega), protein content of the transfected cells were monitored by BCA protein assay kit (Thermo scientific). Transfection experiments with chloroquine (Sigma-Aldrich, 100 μM) were performed as below. The drug was added to the cells 30 min prior to polyplexes addition and polyplexes were exposed to media for 3.5 h, and the medium was changed to serum containing DMEM for an additional 44 h. Then the cells were lysed and assayed by luciferase assay kit and BCA protein assay kit for RLU and protein content, respectively, as described above.

For studying the intracellular trafficking of polyplexes, Hela cells were seeded at 1×10^5 cells/well on sterile cover glasses in a six-well plate. YOYO1-intercalated pDNA was used to prepare polyplexes and added to the cells in serum-free media. Hoechest 33342 and LysoTrackerRed dyes were added 30 min before the incubation termination to stain the nuclei and the acidic vesicles. After 4 h of incubation, the cells were washed twice with PBS and fixed with 4% paraformaldehyde in PBS. The cover glasses were mounted on the slide glasses with a drop of antifade mounting media. The fixed cells were examined under a confocal microscope (FV1000-XY, Olympus) for the detection of the YOYO1-labeled pDNA, Hoechest 33342, and LysoTrackerRed. Fluorescence intensity of YOYO1-intercalated pDNA and red lysotracker was quantified by using ImageJ software.

Statistical Analysis. ANOVA and unpaired Student's *t* test were performed for statistical analysis and $p < 0.01$ considered statistically significant.

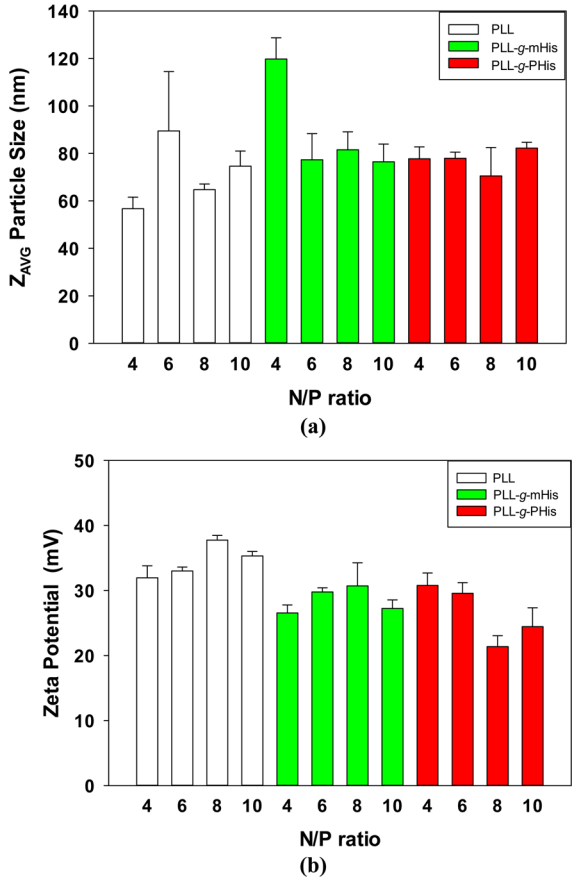

Figure 4. Physicochemical characterization of polyplexes. (a) Particle size and (b) zeta potential of complexes from PLL, PLL-*g*-mHis, and PLL-*g*-PHis with pDNA at different ratios.

RESULTS AND DISCUSSION

Preparation and Characterization of Histidylated PLLs. The chemical structures of PLL-*g*-PHis and PLL-*g*-mHis polymers are shown in Figure 1, and the synthetic schemes and ^{1}H NMR spectra are in Figure S1. The 3.7 kDa PHis with a polydispersity 1.2 was prepared by the same method mentioned in our previous paper,[26] and the GPC curve is provided in Figure S2. As reported previously, the

dx.doi.org/10.1021/bm500843r | *Biomacromolecules* 2014, 15, 3577−3586

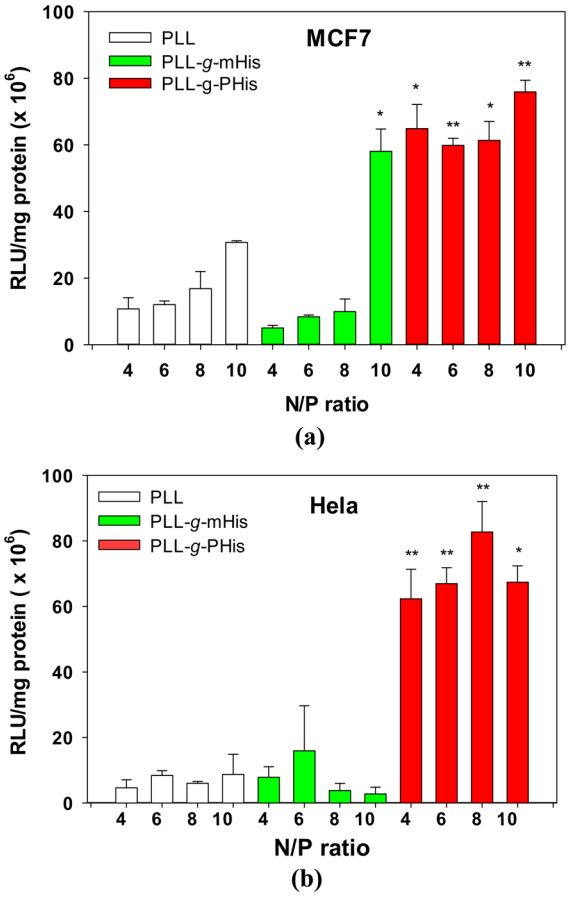

Figure 5. Luciferase expression of polyplexes at various N/P ratios in (a) MCF7 and (b) Hela cells; * and ** means $p < 0.01$ and $p < 0.001$ vs PLL polyplexes (mean ± std error; $n \geq 4$).

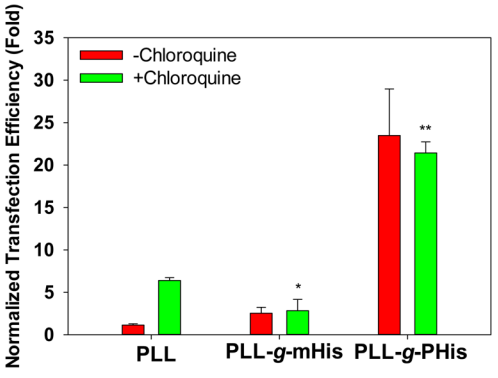

Figure 6. Normalized transfection efficiency of polyplexes in Hela cells (N/P 4). Transfections were performed in the absence (−) and presence (+) of chloroquine. Result expressed as mean ± std error; $n \geq 4$, where *$p < 0.01$ and **$p < 0.001$ compared with (−) CQ.

transfection efficiency of histidylated PLL was optimal with 38 ± 5% of the ε-amino groups in PLL being substituted with histidyl residues.[16] In this study the percentage of total imidazole groups per lysine residue (Lys) was set at 30%.

Buffering Capacity of Polymers in the pH Range. Endosomal escape via the proton sponge effect requires that gene carriers have a high buffering capacity. The buffering capacity of the modified PLL was evaluated as shown in Figure S3 to investigate the change of buffering capacity of PLL upon either mHis or PHis incorporation. As expected, acid-base

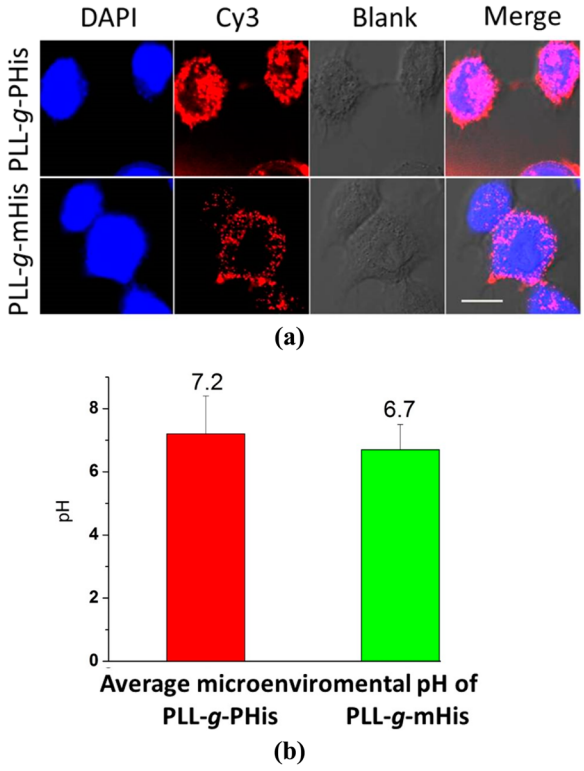

Figure 7. Polymers treated in Hela cells (a) confocal images of PLL-*g*-PHis and PLL-*g*-mHis at 50 μg/mL after a 1.5 h incubation. Scale bar: 20 μm. (b) Intracellular pH of PLL-*g*-PHis and PLL-*g*-mHis at 50 μg/mL after a 1.5 h incubation. Data shown are the mean ± std error; n = 3.

titration revealed that unmodified PLL showed the least buffering capacity, whereas introducing imidazole groups increased the buffering capacity between lysosomal (pH 5) and cytoplasmic (pH 7.2) pH. The buffering capacity of PLL-*g*-PHis was slightly higher than PLL-*g*-mHis though both had an equivalent number of imidazole groups (Figure 1). The higher buffering capacity of PLL-*g*-PHis may be attributed to the short distance between imidazole groups in PHis. The imidazole ring in the His residue contains two ionizable nitrogens (Nδ1 and Nδ2). The pK_a values and the degree of ionization of imidazole rings are influenced by neighboring groups, making them tunable to specific environmental conditions.[37] Titration data also suggests that the pK_a values of the ionizable groups in mHis and PHis are different, which implies that the protonation of the imidazole groups are different depending on the connectivity of His residues. Differential protonation behavior may result from the different distances between imidazole groups in PLL-*g*-mHis and PLL-*g*-PHis. The distance between imidazole groups in PHis is ∼3 Å, whereas, the closest distance in PLL-*g*-mHis is at least 4.5 Å (or even longer), the shorter distance favors more rapid proton transfer via a hydrogen bridge.[38] Multiple adjacent imidazole rings in PHis influence each other and effectively produce an electron rich environment that stabilizes positive charges on imidazole groups and allows higher protonation state.

Hemolysis Activity of Polymers. The pH in the late endosomal compartment ranges from 5 to 6 and from 5 to 5.5 in the lysosomal compartment.[39] The membrane damage should be restricted to endosomal vesicles in a pH-dependent manner, avoiding nonspecific membrane disruption. His

dx.doi.org/10.1021/bm500843r | Biomacromolecules 2014, 15, 3577−3586

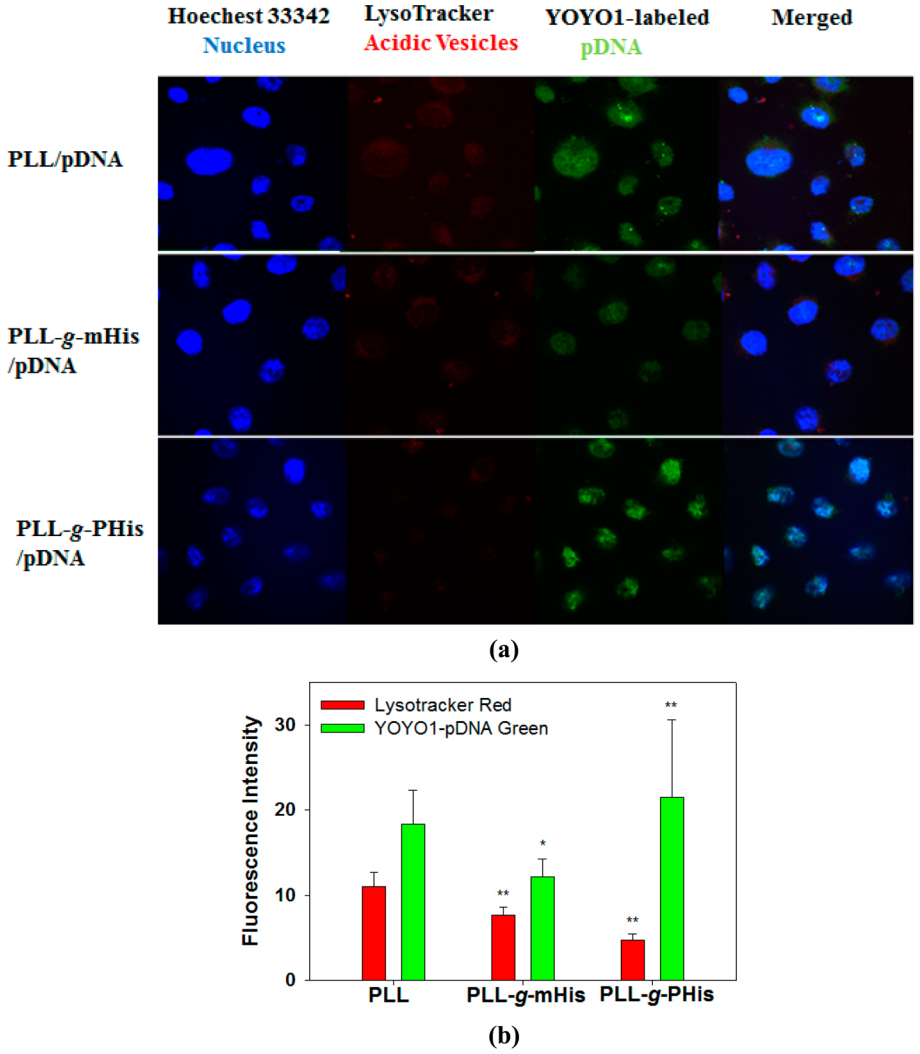

Figure 8. (a) Cellular localization of polyplexes in Hela cells. Confocal images of intracellular distribution of YOYO1-pDNA delivered by polymers; Scale bar 10 μm. (b) Quantification of YOYO1-intercalated pDNA and red lysotracker in the inner-cytoplasm. Results indicate mean ± std error; n = 7, where *p < 0.01 and **p < 0.001 compared with PLL polyplexes.

becomes fully protonated in the endosomal pH range, thus providing pH-responsive membrane destabilizing activity. Though PLL has been widely used as a gene carrier, it shows no apparent pH-dependent hemolysis.[40]

The hemolysis activity of PLL and two His grafted polymers was tested with rabbit red blood cells at two pHs. As shown in Figure 2, PLL at pH 7.4 caused 10% hemolysis, which showed less hemolysis than the His containing polymers. In addition, there was no significant change in the hemolytic activity of PLL as pH dropped from 7.4 to 5.5. This explains PLL is absence of pH-dependent hemolysis. On the other hand, the hemolytic activity of PLL-*g*-mHis changed from 18% at pH 7.4 to 42% at pH 5.5, and PLL-*g*-PHis changed from 27% at pH 7.4 to 75% at pH 5.5. Both histidylated polymers contained an equivalent number of imidazole groups showed pH-responsive membrane disruption, but PLL-*g*-PHis caused more hemolysis at pH 5.5 than PLL-*g*-mHis. Based on the hemolysis assay, PLL-*g*-PHis displayed much higher membrane disruption activity at pH 5.5 compared to PLL-*g*-mHis, making it a potentially better carrier with higher endosome disruption property for gene delivery than PLL-*g*-mHis.

The hemolysis activity appears to be dependent on interactions between the cell membranes and cationic polymers that results local stress on the membrane. In more detail, the hemolytic activity of the polymers is governed by the electrostatic stress force applied to the membrane surface as it swells, and the electrostatic forces produced between the polymers and cell membranes causes a charge imbalance on the membrane. It eventually disrupts the electric fields formed on the RBC membrane to create pores or holes leading to osmotic lysis.[41−43] The external stress forces that destabilize the membrane come from the density of electrostatic interactions of protonated polymers per the membrane surface area,[43] and it has been reported that different protonation states of polymer affect the disruption of RBCs lipid bilayers.[44] The significant difference in hemolytic activity of PHis and mHis suggests that the strength of the stress force induced by PLL-*g*-PHis per the area of the membrane is stronger than that of mHis because the higher charge density on PLL-*g*-PHis at lower pHs produces stronger interactions with the membrane, whereas the more diffuse imidazole groups in PLL-*g*-mHis result in a weaker stress force intensity. Therefore, it is thought that a more protonated state of PLL-*g*-PHis will produce higher electrostatic interactions and induce higher stress forces by interacting more strongly with the membrane, increasing the probability of destabilization and endosomal escape. The observed hemolytic

dx.doi.org/10.1021/bm500843r | *Biomacromolecules* 2014, 15, 3577−3586

activities of pH sensitive polymers show a great potential to disrupt endosomal membranes and aid endosomal escape.[45]

Gel Electrophoresis Study of Polymer/pDNA Complexation. A gel retardation assay was performed to investigate the complexation capability of PLL and PLL-*g*-mHis/PLL-*g*-PHis with pDNA. Polyplexes were prepared at *N*/*P* ratios ranging from 1 to 8 and loaded in agarose gel (Figure 3). Data showed that PLL was able to completely condense genes at *N*/*P* 1, while PLL-*g*-mHis and PLL-*g*-PHis based polyplexes did the same at *N*/*P* 4 and 2, respectively. PLL has a high charge density from primary ε-amino groups, enabling it to condense the genes at a very low *N*/*P* ratio. The ε-amino groups are the histidine grafting sites for both PLL-*g*-mHis and PLL-*g*-PHis, resulting in a lower charge density. Grafted histidine may also pose some steric hindrance to DNA binding. Therefore, complete gene condensation required more PLL-*g*-PHis molecules than PLL and the PLL-*g*-mHis needed even more molecules to condense the same amount of genes since 30% ε-amines in Lys residues are modified with mHis.

To determine the binding strength and stability of polyplexes at different pHs, polyplexes were incubated with increasing concentrations of heparin, which is a competing polyanion with pDNA for the binding to polymers (Figure S4(a)). PLL/pDNA polyplexes remained stable and showed no pH-dependent change of binding strength. In contrast, PLL-*g*-mHis/pDNA and PLL-*g*-PHis/pDNA polyplexes in pH 7.4 buffer required less heparin to expose pDNA compared to PLL/pDNA polyplexes. At pH 5.5, both polyplexes were more resistant to dissociation upon heparin incubation, because the more protonated state of the imidazole groups enhances interactions with pDNA and forms more stable polyplexes. As shown in Figure S4(b), PLL-*g*-PHis/pDNA polyplexes revealed more change in the DNA binding strength as pH drops, indicating that the higher degree of protonation is due to the more fully protonated imidazole groups. The results suggest that decomplexation of histidylated polyplexes provides pH-dependent pDNA release. This will prevent premature pDNA release and effectively protect genes against enzymatic (nuclease) degradation.[46,47] Thus, the different binding strength between PLL-*g*-mHis and PLL-*g*-PHis will influence pDNA release kinetics and plays a critical role in determining transfection efficiency after endosomal escape.

Particle Size and Zeta Potential Profiles of Polyplexes at Various *N*/*P* Ratios. PLL-*g*-PHis formed a micelle at physiological pH because of the amphiphilicity of the polymer. The average diameter of PLL-*g*-PHis in HEPES buffer at pH 7.4 was about 60 nm (Figure S5). The size of micelles increased as the pH dropped and grew sharply at pH 4.5 as the micelles became sufficiently protonated to cause dissociation. To characterize complexation with pDNA, the particle size and zeta potential were monitored at various N/P ratios ranging from 4 to 10 (Figure 4). PLL polyplexes showed the smallest particle size (60−90 nm), whereas, PLL-*g*-mHis and PLL-*g*-PHis were larger (80−120 nm and 70−80 nm, respectively). The size and charge of the polyplexes depends on the number of free primary amino groups on the PLL backbone which can alter the electrostatic interactions with the genes. Thus, PLL can make a compact particle, but this in turn retards the dissociation between PLL and pDNA once located inside the cells and leads to low transfection efficiency.[48]

Cell Viability Analysis Using MTT Assay. Grafting His into PLL reduces the cytotoxicity of the polymer, as assessed in MCF7 and Hela cells using an MTT assay (Figure S6). The cytotoxicity of PLL was significantly higher in both cell lines, but PLL-*g*-mHis and PLL-*g*-PHis showed negligible cytotoxicity within the tested concentration range. The difference between PLL and PLL grafted with histidine is mainly due to the reduced numbers of free ε-amines. Since 30 Lys residues are grafted with mHis in PLL-*g*-mHis, it has the lowest surface charge and the highest cell viability of the three polymers followed by PLL-*g*-PHis and PLL. This MTT data suggests that the hemolytic activity of PLL-*g*-PHis was induced by a pH sensitive mechanism at pH 5.5 without compromising cell viability. Thus, PLL-*g*-PHis becomes more protonated at lower pH, and strongly interacts with the RBCs membrane where it causes membrane disruption.

In Vitro Transfection Efficiency Evaluation of Polyplexes. The in vitro transfection efficiency of the genes carried by PLL-*g*-mHis and PLL-*g*-PHis was compared to PLL using a luciferase activity in MCF7 (Figure 5a) and Hela cells (Figure 5b). PLL-*g*-mHis/pDNA polyplexes in MCF7 cells had lower transfection efficiency than PLL up to N/P 8, but the efficiency was enhanced about 2-fold at *N*/*P* 10 with statistical significance ($p < 0.01$); however, 6.5-fold higher gene expression was observed with PLL-*g*-PHis/pDNA than PLL, even at *N*/*P* 4. In Hela cells, both PLL-*g*-mHis (statistically not significant) and PLL-*g*-PHis showed enhanced transfection efficiency compared to PLL. mHis modification resulted in a minor improvement in luciferase activity without statistical significance ($p = 0.32$), but PHis showed up to a 10-fold enhancement in transfection efficiency even at the lowest *N*/*P* ratio ($p < 0.001$). Incorporation of histidine groups enhanced luciferase activity by providing buffering capacity in PLL, but the degree to which transfection efficiency improves depends on the arrangement of imidazole groups. PLL-*g*-mHis requires more polymer per quantity of gene (higher *N*/*P* ratio) than other polymers, because there are fewer ε-amines available for gene interactions due to the substitution of histidine monomers on the PLL backbone. Higher transfection efficiency compared to PLL and PLL-*g*-mHis was observed via PLL-*g*-PHis, since PHis can provide stronger endosomolytic activity during transfection, as was demonstrated in the hemolysis assay (Figure 2). We conclude that given an equivalent number of histidine residues attached to PLL for buffering capacity, PHis grafting provided better performance in terms of endosomal disruption and transfection efficiency.

Since the final transfection efficiency levels are strongly associated with the ability of polyplexes to escape the endosome, transfection of the polyplexes was evaluated with the treatment of chloroquine (CQ) to evaluate the ability of polyplexes to escape from the endosomes in Hela cells (Figure 6). CQ is a weak base endosomolytic agent that mainly accumulates in the late endosome and lysosomes, and causes a reduction of protonation. Thus, CQ acts as a proton buffer and enhances the release of genes into the cytoplasm.[49] As shown in Figure 6, the presence of CQ enhanced the transfection efficiency of PLL/pDNA polyplexes by bolstering the weak endosomolytic activity of PLL. PLL-*g*-mHis/pDNA transfection activity was slightly boosted by CQ, because it was able to escape the endosomes on its own but slowly. On the other hand, the preincubation of CQ did not enhance the transfection efficiency of PLL-*g*-PHis/pDNA. We can conclude PLL-*g*-PHis helps pDNA escape into the cytoplasm from the early endosomes before the gene degradation in the late endosome or lysosomal phases occurs.

Scheme 1. Schematic Illustration of a Local Stress Development by Interactions between the PLL-*g*-mHis/PLL-*g*-PHis and the Endosomal Membrane

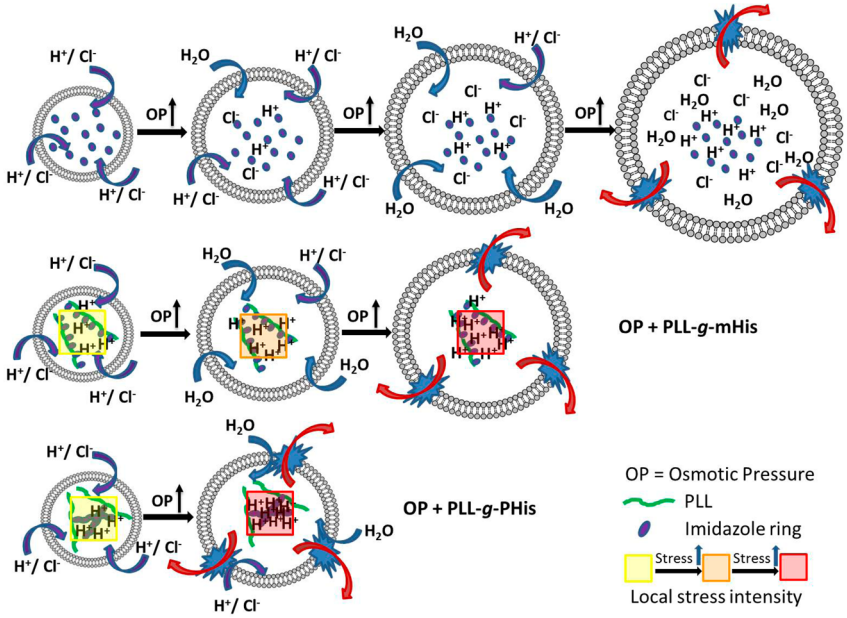

Intracellular Localization and pH Environment of the Polymers. To investigate the impact of the polymers inside the cell, confocal microscopy and flow cytometry were used to track intracellular localization and pH environment of the polymers in the cells. As shown in Figure 7a, Cy3-labeled PLL-*g*-PHis and PLL-*g*-mHis yielded discernible localization results after 1.5 h incubation. After a 1.5 h incubation, PLL at a concentration of 50 μg/mL killed most of the cells due to high polymer toxicity. It was obvious that the Cy3 red from PLL-*g*-mHis was mostly located around the cell nucleus, whereas a higher portion of red fluorescence was found inside of the nucleus for PLL-*g*-PHis. Interestingly, PLL-*g*-PHis was able to translocate inside the nucleus, which is an advantage for gene delivery and gene expression. The fluorescence intensity ratio of pH-sensitive and pH-insensitive dyes is linearly related to the pH environment of the labeled polymers. After conjugation with Cy3 (pH-insensitive) and FITC (pH-sensitive), flow cytometry data (Figure 7b) demonstrated that the average pH around PLL-*g*-mHis was pH 6.7, suggesting that most polymer molecules are trapped in the early endosomes (pH 5.5−6.5).[39] However, the average pH, where PLL-*g*-PHis located was 7.2, implying that the polymer escaped from the endosomal/lysosomal compartments and entered into the cytoplasm and nucleus (pH 7.2) after a 1.5 h incubation. In more detail, the narrow time points of PLL-*g*-PHis were monitored to track the fluorescence changes over time. As shown in Figure S7, after 0.5 and 1 h incubation, the fluorescence was located around the cell nucleus, and after a 1.5 h incubation, most of the fluorescence translocated into the nucleus. The pH remained almost the same for the first 1 h (pH 6.7−6.8) and slightly changed to 7.2 after 1.5 h, which not only confirmed the endosomal escape of PLL-*g*-PHis, but also showed the exact time point when PLL-*g*-PHis escapes from the acidic compartment, while PLL-*g*-mHis was still entrapped. This observation is the evidence of the powerful membrane disruption and cell permeability ability of PLL-*g*-PHis.

Intracellular Localization of pDNA Delivered by Polymers. To verify efficient functional transfection by the His-grafted PLL, Hela cells were treated with the polyplexes carrying YOYO1-pDNA at *N*/*P* 4, and the intracellular localization of the fluorescently tagged DNA was monitored for each polymer. As shown in Figure 8a, the results indicated that the YOYO1-pDNA from PLL polyplexes was localized in both the nucleus and cytoplasm, and red lysotracker staining was more intense in the cells treated with PLL/pDNA than in PLL-*g*-mHis/pDNA or PLL-*g*-PHis/pDNA. A large amount of green fluorescence was colocalized with red lysotracker, which implies that a significant fraction of PLL/pDNA complexes are trapped inside the acidic compartments. The lack of proton buffering and endosomal membrane rupturing ability prevented the release of polyplexes from the endosome, thus, the localized polyplexes in the endosomes are trafficked to the lysosomes and degraded, leading to low transfection efficiency.[50] The intracellular intensity of YOYO1-pDNA (Figure 8b) delivered by PLL-*g*-mHis polyplexes was lower than other polyplexes at 4 h post-transfection, probably because it has the lowest surface charge; however, YOYO1-pDNA was more localized in the nucleus than in the cytoplasm, and lower lysotracker intensity was observed in mHis-grafted PLL than in PLL polyplexes due to the proton buffering capacity that lead to greater release of polyplexes from the endosomes. The results support that the endosomolytic activity by mHis grafting plays a more important role than cellular uptake in transfection efficiency (Figure S8). The experiment with PLL-*g*-PHis polyplexes revealed that significant quantities of YOYO1-pDNA were translocated inside the nucleus and the polyplexes were barely detected in the acidic vesicles of the cell. The cluster of imidazole rings in PLL-*g*-PHis provided even higher endosomolytic activity than PLL-*g*-mHis, which lead to stronger endosomal membrane destabilization and favored quick endosomal escape.

CONCLUSION

Both mHis and PHis grafting enhanced the buffering capacity of PLL, but despite having an equivalent number of imidazole groups, the two polymer architectures have different buffering capacity and gene transfection efficiency. More importantly,

dx.doi.org/10.1021/bm500843r | *Biomacromolecules* 2014, 15, 3577−3586

PLL-*g*-PHis containing imidazole rings in polymer form showed significantly stronger endosomolytic activity than that from PLL-*g*-mHis. This difference is due to higher local charge density at endosomal pH, which creates a stronger electrostatic stress force and interacts to a greater extent with the endosomal membrane (Scheme 1). This dense ionic interactions result in greater local electrostatic stresses on the membrane as the endosome swells from the osmotic pressure build-up caused by the imidazole groups buffering capacity. The localized stress facilitates membrane destabilizing activity via a combination of increased osmotic potential due to the polymer buffering capacity and direct interactions with the membrane, as evidenced by improved hemolytic activity of PLL-*g*-PHis. This indicates that the ionization behavior of polymers depends on the architecture and may change the local stress intensity on the membrane and significantly contribute to endosomal disrupting activity. Thus, we conclude that the pH-sensitive polymeric endosomolytic agents (PLL-*g*-PHis) are more effective in gene transfer than monomeric and scattered counter parts (PLL-*g*-mHis), and results in enhanced transfection efficiency. In addition, grafting PHis to the PLL backbone lowered the cytotoxicity at the cost of a minimal reduction of free amines in PLL, resulting in slightly lowered gene condensation capability and a higher cellular uptake than mHis. Therefore, improved endosomal escape resulted in the highest intracellular localization in the nucleus as well as effective gene transfection.

■ ASSOCIATED CONTENT

Supporting Information

Details about the synthetic schemes of polymers and ^{1}H NMR analysis; GPC of PHis; Acid−base titration; pH-dependent pDNA release using a heparin competition assay; The particle size changes of PLL-*g*-PHis upon pH changes; Dose-dependent cytotoxicity of polymers in MCF7 and Hela cells; Confocal images of PLL-*g*-PHis at different time points; Cellular uptake of polyplexes in Hela cells. This material is available free of charge via the Internet at http://pubs.acs.org.

■ AUTHOR INFORMATION

Corresponding Author

*Tel.: +1-801-585-1518. Fax: +1-801-585-3614. E-mail: you.bae@utah.edu.

Author Contributions

†These authors equally contributed to this work (H.S.H. and J.H.).

Notes

The authors declare no competing financial interest.

■ ACKNOWLEDGMENTS

This work was supported by NIH GM82866. We appreciate Joseph Nichols (The University of Utah) for thoughtful comments and helpful corrections.

■ REFERENCES

(1) Gruenberg, J.; van der Goot, F. G. *Nat. Rev. Mol. Cell Biol.* **2006**, *7*, 495−504.

(2) Lee, Y.; Miyata, K.; Oba, M.; Ishii, T.; Fukushima, S.; Han, M.; Koyama, H.; Nishiyama, N.; Kataoka, K. *Angew. Chem.* **2008**, *120*, 5241−5244.

(3) Convertine, A.; Diab, C.; Prieve, M.; Paschal, A.; Hoffman, A.; Johnson, P.; Stayton, P. *Biomacromolecules* **2010**, *11*, 2904−2911.

(4) Gu, W.; Jia, Z.; Truong, N. P.; Prasadam, I.; Xiao, Y.; Monteiro, M. J. *Biomacromolecules* **2013**, *14*, 3386−3389.

(5) Rehman, Z. u.; Hoekstra, D.; Zuhorn, I. S. *ACS Nano* **2013**, *7*, 3767−3777.

(6) Kim, T. H.; Ihm, J. E.; Choi, Y. J.; Nah, J. W.; Cho, C. S. *J. Controlled Release* **2003**, *93*, 389−402.

(7) Yamagata, M.; Kawano, T.; Shiba, K.; Mori, T.; Katayama, Y.; Niidome, T. *Bioorg. Med. Chem.* **2007**, *15*, 526−532.

(8) Cho, Y. W.; Kim, J. D.; Park, K. *J. Pharm. Pharmacol.* **2003**, *55*, 721−734.

(9) Putnam, D.; Gentry, C. A.; Pack, D. W.; Langer, R. *Proc. Natl. Acad. Sci. U.S.A.* **2001**, *98*, 1200−1205.

(10) Funhoff, A. M.; van Nostrum, C. F.; Koning, G. A.; Schuurmans-Nieuwenbroek, N. M.; Crommelin, D. J.; Hennink, W. E. *Biomacromolecules* **2004**, *5*, 32−39.

(11) Leroueil, P. R.; Berry, S. A.; Duthie, K.; Han, G.; Rotello, V. M.; McNerny, D. Q.; Baker, J. R.; Orr, B. G.; Banaszak Holl, M. M. *Nano Lett.* **2008**, *8*, 420−424.

(12) Griffiths, P.; Paul, A.; Khayat, Z.; Wan, K.-W.; King, S.; Grillo, I.; Schweins, R.; Ferruti, P.; Franchini, J.; Duncan, R. *Biomacromolecules* **2004**, *5*, 1422−1427.

(13) Benjaminsen, R. V.; Mattebjerg, M. A.; Henriksen, J. R.; Moghimi, S. M.; Andresen, T. L. *Mol. Ther.* **2013**, *21*, 149−157.

(14) Richard, I.; Thibault, M.; De Crescenzo, G.; Buschmann, M. D.; Lavertu, M. *Biomacromolecules* **2013**, *14*, 1732−1740.

(15) Midoux, P.; Monsigny, M. *Bioconjugate Chem.* **1999**, *10*, 406−411.

(16) Pack, D. W.; Putnam, D.; Langer, R. *Biotechnol. Bioeng.* **2000**, *67*, 217−223.

(17) Boeckle, S.; Fahrmeir, J.; Roedl, W.; Ogris, M.; Wagner, E. *J. Controlled Release* **2006**, *112*, 240−248.

(18) Singh, R. S.; Gonçalves, C.; Sandrin, P.; Pichon, C.; Midoux, P.; Chaudhuri, A. *Chem. Biol.* **2004**, *11*, 713−723.

(19) Fielden, M. L.; Perrin, C.; Kremer, A.; Bergsma, M.; Stuart, M. C.; Camilleri, P.; Engberts, J. B. *Eur. J. Biochem.* **2001**, *268*, 1269−1279.

(20) Shi, J.; Schellinger, J. G.; Johnson, R. N.; Choi, J. L.; Chou, B.; Anghel, E. L.; Pun, S. H. *Biomacromolecules* **2013**, *14*, 1961−1970.

(21) Chang, K.-L.; Higuchi, Y.; Kawakami, S.; Yamashita, F.; Hashida, M. *Bioconjugate Chem.* **2010**, *21*, 1087−1095.

(22) Lee, E. S.; Gao, Z.; Bae, Y. H. *J. Controlled Release* **2008**, *132*, 164−170.

(23) Lee, E. S.; Na, K.; Bae, Y. H. *Nano Lett.* **2005**, *5*, 325−329.

(24) Lee, E. S.; Na, K.; Bae, Y. H. *J. Controlled Release* **2005**, *103*, 405−418.

(25) Lee, E. S.; Shin, H. J.; Na, K.; Bae, Y. H. *J. Controlled Release* **2003**, *90*, 363−374.

(26) Hu, J.; Miura, S.; Na, K.; Bae, Y. H. *J. Controlled Release* **2013**, *172*, 69−76.

(27) Kim, D.; Lee, E. S.; Park, K.; Kwon, I. C.; Bae, Y. H. *Pharm. Res.* **2008**, *25*, 2074−2082.

(28) Oh, K. T.; Yin, H.; Lee, E. S.; Bae, Y. H. *J. Mater. Chem.* **2007**, *17*, 3987−4001.

(29) Lv, H.; Zhang, S.; Wang, B.; Cui, S.; Yan, J. *J. Controlled Release* **2006**, *114*, 100−109.

(30) Hwang, H. S.; Kang, H. C.; Bae, Y. H. *Biomacromolecules* **2013**, *14*, 548−556.

(31) Wiethoff, C. M.; Middaugh, C. R. *J. Pharm. Sci.* **2003**, *92*, 203−217.

(32) Kang, H. C.; Huh, K. M.; Bae, Y. H. *J. Controlled Release* **2012**, *164*, 256−264.

(33) Kang, H. C.; Kang, H.-J.; Bae, Y. H. *Biomaterials* **2011**, *32*, 1193−1203.

(34) Lackey, C. A.; Murthy, N.; Press, O. W.; Tirrell, D. A.; Hoffman, A. S.; Stayton, P. S. *Bioconjugate Chem.* **1999**, *10*, 401−405.

(35) Kang, H. C.; Samsonova, O.; Bae, Y. H. *Biomaterials* **2010**, *31*, 3071−3078.

(36) Fichter, K. M.; Ingle, N. P.; McLendon, P. M.; Reineke, T. M. *ACS Nano* **2012**, *7*, 347−364.

(37) Sachs, D. H.; Schechter, A. N.; Cohen, J. S. *J. Biol. Chem.* **1971**, *246*, 6576−6580.
(38) Song, X. j.; McDermott, A. E. *Magn. Reson. Chem.* **2001**, *39* (S1), S37−S43.
(39) Kang, H. C.; Lee, M.; Bae, Y. H. *Crit. Rev. Eukaryotic Gene Expression* **2005**, *15*, 317−342.
(40) Ferruti, P.; Manzoni, S.; Richardson, S. C.; Duncan, R.; Pattrick, N. G.; Mendichi, R.; Casolaro, M. *Macromolecules* **2000**, *33*, 7793−7800.
(41) Chen, R.; Khormaee, S.; Eccleston, M. E.; Slater, N. K. *Biomaterials* **2009**, *30*, 1954−1961.
(42) Sovadinova, I.; Palermo, E. F.; Huang, R.; Thoma, L. M.; Kuroda, K. *Biomacromolecules* **2010**, *12*, 260−268.
(43) Jean-François, F.; Elezgaray, J.; Berson, P.; Vacher, P.; Dufourc, E. J. *Biophys. J.* **2008**, *95*, 5748−5756.
(44) Choudhury, C. K.; Kumar, A.; Roy, S. *Biomacromolecules* **2013**, *14*, 3759−3768.
(45) Bulmus, V.; Woodward, M.; Lin, L.; Murthy, N.; Stayton, P.; Hoffman, A. *J. Controlled Release* **2003**, *93*, 105−120.
(46) Boylan, N. J.; Kim, A. J.; Suk, J. S.; Adstamongkonkul, P.; Simons, B. W.; Lai, S. K.; Cooper, M. J.; Hanes, J. *Biomaterials* **2012**, *33*, 2361−2371.
(47) Zhou, D.; Li, C.; Hu, Y.; Zhou, H.; Chen, J.; Zhang, Z.; Guo, T. *J. Mater. Chem.* **2012**, *22*, 10743−10751.
(48) Parelkar, S. S.; Chan-Seng, D.; Emrick, T. *Biomaterials* **2011**, *32*, 2432−2444.
(49) Akinc, A.; Thomas, M.; Klibanov, A. M.; Langer, R. *J. Gene Med.* **2005**, *7*, 657−663.
(50) Kang, H. C.; Bae, Y. H. *Adv. Funct. Mater.* **2007**, *17*, 1263−1272.